

Full Length Article

High speed cutting of AZ31 magnesium alloy

Liwei Lu ^{a,b,*}, Shaohua Hu ^a, Longfei Liu ^{a,**}, Zhenru Yin ^a

^a College of Mechanical and Electrical Engineering, Hunan University of Science and Technology, Xiangtan 411201, Hunan, China

^b School of Materials Science and Engineering, Central South University, Changsha 410083, Hunan, China

Received 2 April 2016; revised 20 April 2016; accepted 26 April 2016

Available online 9 May 2016

Abstract

Using LBR-370 numerical control lathe, high speed cutting was applied to AZ31 magnesium alloy. The influence of cutting parameters on microstructure, surface roughness and machining hardening were investigated by using the methods of single factor and orthogonal experiment. The results show that the cutting parameters have an important effect on microstructure, surface roughness and machine hardening. The depth of stress layer, roughness and hardening present a declining tendency with the increase of the cutting speed and also increase with the augment of the cutting depth and feed rate. Moreover, we established a prediction model of the roughness, which has an important guidance on actual machining process of magnesium alloy.

© 2016 Production and hosting by Elsevier B.V. on behalf of Chongqing University. This is an open access article under the CC BY-NC-ND license (<http://creativecommons.org/licenses/by-nc-nd/4.0/>).

Keywords: AZ31 magnesium alloy; High speed cutting; Cutting parameters; Hardening; Roughness; Stress layer

1. Introduction

Magnesium alloy has many advantages, such as high strength-to-weight, high stiffness-to-weight ratios, and no pollution, etc., so it has a very broad application prospect, and thus it was called green metal material in 21st century [1–3]. As for today's energy crisis, it is urgent to accelerate the development of magnesium materials. Nowadays, the current research of magnesium alloy mostly focus on plastic processing technology (e.g. forging, extrusion, rolling, drawing, stamping) and heat treatment (e.g. annealing, solid solution and aging) [4–7]. Machining (e.g. cutting, turning, milling) is one of the basic manufacturing processes usually found in fabrication of components and structures [8]. However, the research about high speed cutting of magnesium alloy is very few. The tools about cutting steels and other alloys have been commonly reported in previous reports [9,10], the temperature variation during the

cutting process was referred [11], the optimization of surface roughness and cutting force were also studied [12,13], and how the cutting parameters affect cutting chip, roughness and residual stress were further studied [14,15]. However, the high speed cutting of Mg alloys still lacks systematic study and deepen analysis.

In this work, we carried out a series of experiment to systematically reveal the effect of cutting parameters on the microstructure, residual stress, hardening behavior, and roughness of AZ31B Mg alloys. Combing the analysis of microstructure and vickers hardness, the residual stress distribution after high speed cutting was discussed. Meanwhile, the roughness was measured to reflect the surface quality of workpiece, and the new predicted model of roughness was established.

2. Materials and experimental procedures

The materials used in this study were commercial AZ31 magnesium alloy; the main ingredients was shown in Table 1.

The size of cutting billets was $\Phi 23$ mm \times 200 mm, which were machined from the extruded AZ31 Mg alloys with a diameter of $\Phi 23$ mm and a length of 1000 mm. High speed cutting was conducted on LBR-370 numerical control lathe, and the material of cutting tool with 15 mm in length and 15 mm in width and 5 mm in thickness used was YT15, and the cutting edge angle was 6° , the cutting edge radius r was 0.2 mm, and

* Corresponding author. College of Mechanical and Electrical Engineering, Hunan University of Science and Technology, Xiangtan 411201, Hunan, China. Tel.: +86 731 5829 0847; fax: +86 731 5829 0847.

E-mail address: cqullw@163.com (L. Lu)

** Corresponding author. College of Mechanical and Electrical Engineering, Hunan University of Science and Technology, Xiangtan 411201, Hunan, China. Tel.: +86 731 5829 0480; fax: +86 731 5829 0480.

E-mail address: lffiu1@hnust.edu.cn (L. Liu).

Table 1
Chemical composition of the AZ31 magnesium alloy.

Element		Al	Zn	Mn	Si	Cu	Ni	Fe
Wt%	min	2.5	0.6	0.2				
	max	3.5	1.4	1.0	0.1	0.05	0.005	0.005

Table 2
Cutting parameters of the AZ31 magnesium alloy.

Order number	Speed (r/min)	Ap (mm)	F (mm/r)
1	1000	1	0.05
2	1400	1	0.05
3	1800	1	0.05
4	2200	1	0.05
5	1400	0.5	0.05
6	1400	1	0.05
7	1400	1.5	0.05
8	1400	2	0.05
9	1400	1	0.02
10	1400	1	0.05
11	1400	1	0.08
12	1400	1	0.11

the rear angle was 9° . The cutting parameters were listed in Table 2. It should be noted that all the cutting length was 20 mm.

Surface roughness was measured by a portable surface roughness equipment (LINKS-HOMMLET1000). Five points were selected from each cutting surface, and their average value was calculated to be roughness value. After that, the optical microscopy (OM) observations of cross section were carried out, and the observation samples were machined from the plane of cross section, which can be seen from Fig. 1. The OM samples were prepared by polishing surface mechanically and etching in a solution of 10 ml acetic acid, 4.2 g picric acid, 10 ml water, and 70 ml ethanol. Finally, the hardness of cross section was measured from edge to internal, and the distance between two adjacent points was $5 \mu\text{m}$. The Hv was measured over ten successful readings for each sample using a digital tester DMH-1 (Matsuzawa Seiki Co., Ltd.), the indenter load and holding time at test pressure were 100 g and 8 s, respectively.

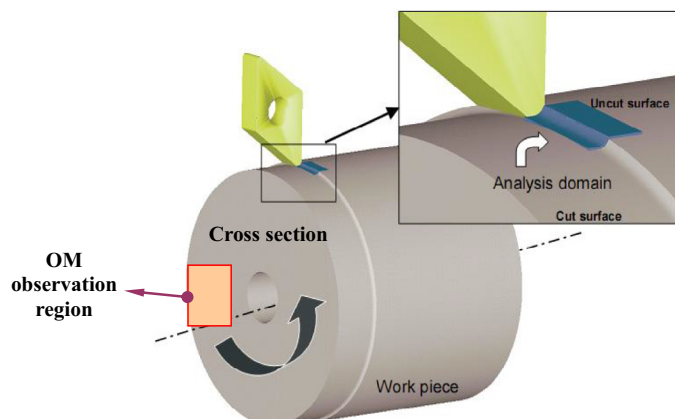


Fig. 1. Schematic of the cutting method and OM observation region.

3. Results and discussion

3.1. Microstructure

The original microstructure of the work piece is shown in Fig. 2. Many coarse and tiny grains are observed. The size of some coarse grains reaches up to $150 \mu\text{m}$, and the tiny grain size is about $6 \mu\text{m}$. It is statistically found that a large amount of grain size is measured to be between $50 \mu\text{m}$ and $100 \mu\text{m}$.

From the Fig. 3, there is an obvious stress layer at the edge of the cross section of cutting product, and the stress layer depth decreases from $40 \mu\text{m}$ to $25 \mu\text{m}$ with the increase of cutting speed from 1000 r/min to 2200 r/min. Careful observation reveals that the number of crystal twins also presents a decreasing tendency with the increase of the cutting speed, which can be attributed to the contacted time between the tool and the work piece reduces with the increase of the cutting speed, and the stress layer gets small, imposing an important effect on the time of interaction force between the tool and the work piece, thus preventing the formation of the residual stress in the surface of the work piece. There are some reasons for this special residual stress: (1) as for the high speed cutting process, the density of the work piece is mainly affected by the surface variation, and the high speed cutting can easily increase the surface temperature, which decreases the tendency of residual stress on the surface of work piece. From Fig. 3a, one can see that many slim twins come out. However, the number of them is gradually reduced for the effect of increasing temperature with the increase of cutting speed (Fig. 3b–d). (2) The cutting surface is subjected to severe plastic deformation under the action of cutting force, after the cutting completion, a large amount of work hardening remains, resulting in serious residual stress in the work piece surface [16].

From the Fig. 4, as the cutting depth increases from 0.5 mm to 2 mm, there are no great changes for the stress layer depth of the work piece. As for the work piece with 0.5 mm and 1 mm cutting depth, the stress layer depth are measured to be about $20 \mu\text{m}$ and $25 \mu\text{m}$, respectively (Fig. 4a and b). It is interesting to find that the same stress layer depth comes out for the work piece with 1.5 mm and 2 mm cutting depth, indicating that the influence of cutting depth on the stress layer depth is not

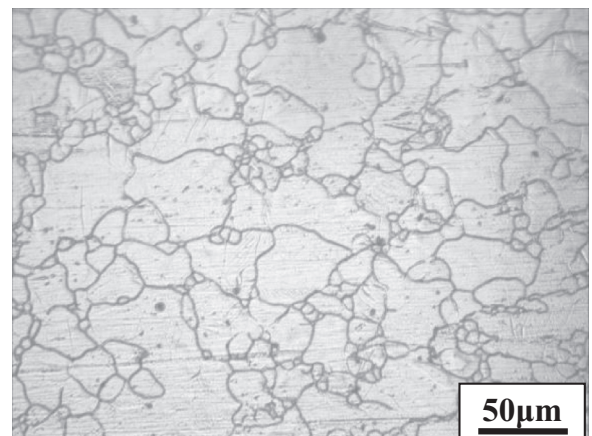


Fig. 2. Microstructure of AZ31 Mg alloys before cutting process.

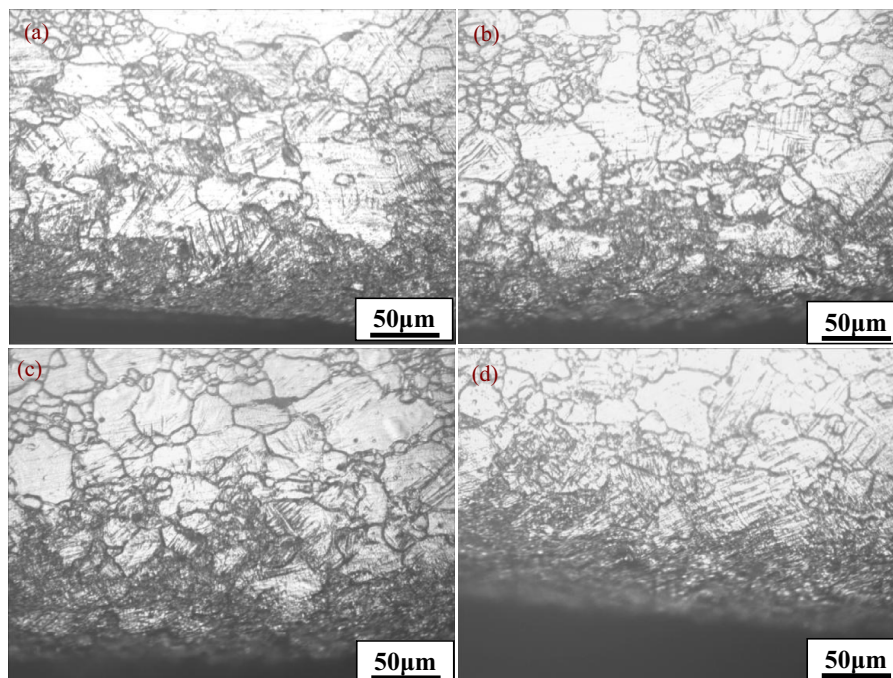


Fig. 3. Microstructure of AZ31 Mg alloys after cutting process at different cutting speed: (a) 1000 r/min; (b) 1400 r/min; (c) 1800 r/min; and (d) 2200 r/min. ($a_p = 1$ mm, $f = 0.05$ mm/r).

obvious. Since the relatively low hardness of magnesium alloy, the high processing index and the small energy consumption, AZ31 Mg alloys could achieve cutting processing with large dosage. Besides, the effect of cutting depth on the cutting parameters such as cutting force, cutting temperature rise and so on is also not obvious. Therefore, the stress layer depth has no obvious change with the variation of cutting depth.

To further reveal the effect of feed rate on the stress layer depth, we present Fig. 5. With the increase of feed rate from 0.02 to 0.08, the change of stress layer depth is not obvious, and the value increases from 10 μm to 25 μm . However, the stress layer depth for the feed rate of 0.11 can reach up to 40 μm , suggesting that the stress layer depth has no significant changes for the feed rate increased in a small range, while the

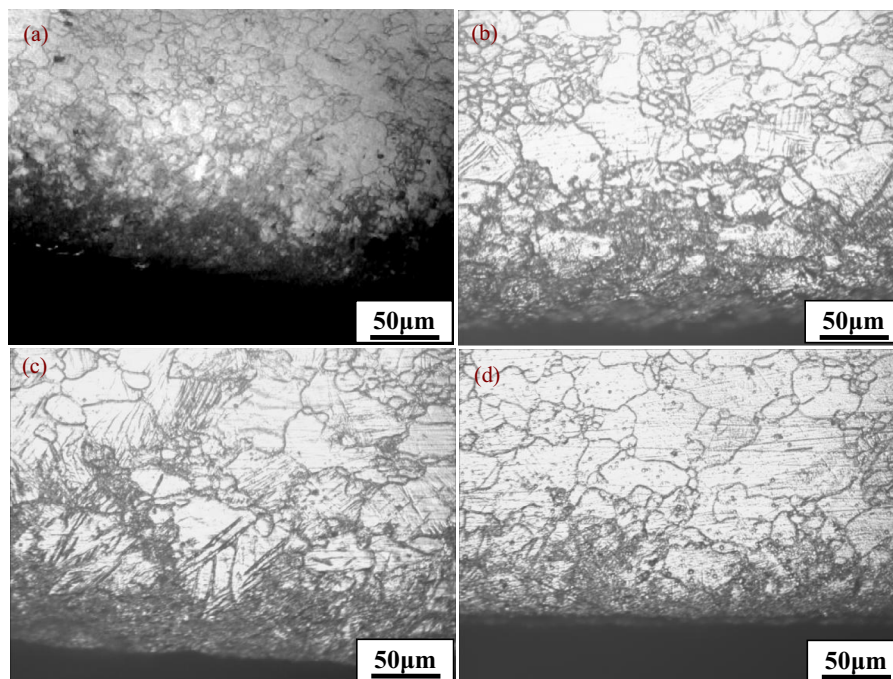


Fig. 4. Microstructure of AZ31 Mg alloys after cutting process at different cutting depth: (a) 0.5 mm; (b) 1 mm; (c) 1.5 mm; and (d) 2 mm. ($v = 1400$ r/min, $f = 0.05$ mm/r).

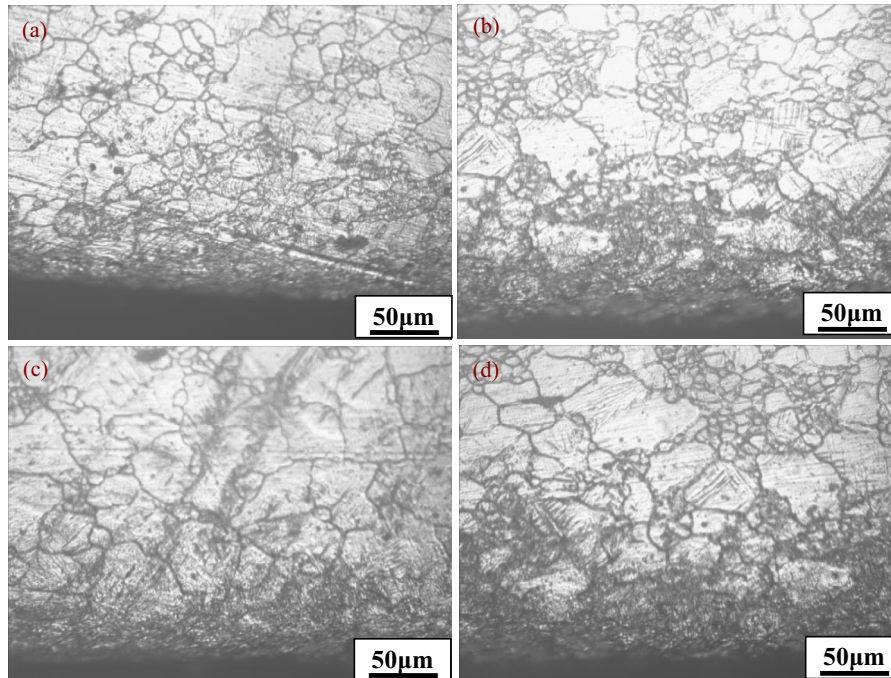


Fig. 5. Microstructure of AZ31 Mg alloys after cutting process at different feed rate: (a) 0.02 mm/r; (b) 0.05 mm/r; (c) 0.08 mm/r; and (d) 0.11 mm/r. ($v = 1400$ r/min, $a_p = 1$ mm).

feed rate increases to a certain extent, the stress layer depth will get much larger. Since for the condition of large feed rate, the removal rate of work piece is greatly improved in unit time, and thermal effect strengthens, thus playing a leading role, which make large heat generated in the cutting process and gathered in the surface layer of the work piece, thus the surface material will expand largely, but it is prevented by their surrounding material, so the heat stress turns into residual stress.

3.2. Hardness

Fig. 6 shows the hardness variation in the cross section with the increase of cutting speed. Each curve presents a gradual downward trend from the edge to internal. As the cutting speed

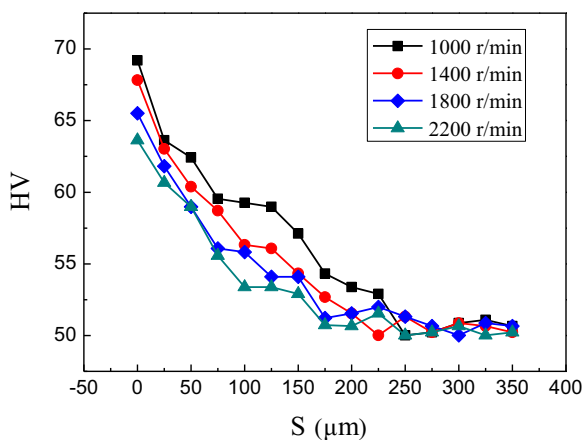


Fig. 6. Effect of cutting speed on the hardness of AZ31 Mg alloys. ($a_p = 1$ mm, $f = 0.05$ mm/r).

increases from 1000r/min to 2200r/min, the hardening ability decreases from about 135% to 120%, which can be attributed to the hardening degree of the surface of work piece that mainly depends on the plastic deformation and cutting heat. During the cutting process, the plastic deformation makes the lattice distorted and crushed, resulting in serious hardening behavior, while deformation heat causes thermal softening in the surface. With the increase of cutting speed, the temperature also increases, which will enhance the thermal softening effect. The increasing temperature makes the flow stress decreased, and the dislocation density come down according to the dislocation theory, that is, the hardening caused by the dislocation decreases. So, the surface hardening reduces with the increase of the cutting speed in a certain speed range. When the distance is greater than 200 μm , the hardening effect is not obvious, so the hardness will no longer change.

The hardness variation with different cutting depth at cross section from the edge to interior is shown in Fig. 7. Generally, each curve shows a decreasing trend, and in some local regions, the hardness increases, which may be caused by the uneven microstructure of the original billet. From the curve, the hardening ability increases as the cutting depth increases. As for the 0.5 mm cutting depth, the hardening ability was about 125%, while it increases to about 140 for the 2 mm cutting depth. With the increase of cutting depth, the cutting force improves, and the squeezing effect of tool on work piece becomes very strong, so the plastic deformation of the work piece surface strengthens. In addition, due to the material removal rate increases, resulting in the decrease of heat quantity removed by the chip; therefore, the hardening effect becomes obvious.

Fig. 8 shows the hardness variation with different cutting feed at cross section from the edge to interior. The work

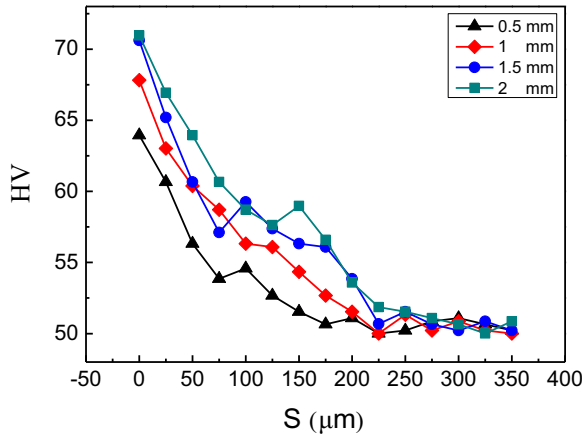


Fig. 7. Effect of cutting depth on the hardness of AZ31 Mg alloys. (V = 1400 r/min, f = 0.05 mm/r).

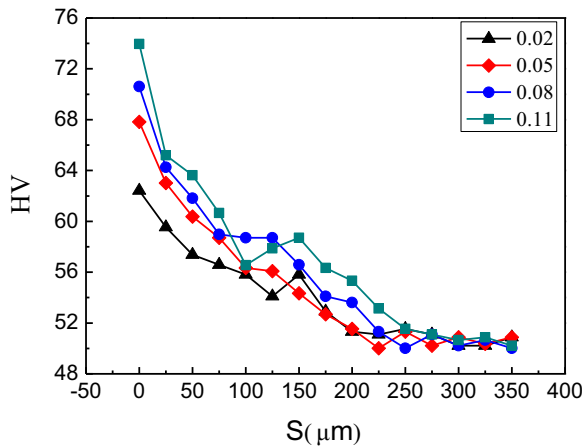


Fig. 8. Effect of feed rate on the hardness of AZ31 Mg alloys. (V = 1400 r/min, ap = 1 mm).

hardening of surface increases with the increase of feed rate. As for the 0.02 mm/r feed rate, the hardening ability is about 120%, while it increases to about 145% with the feed rate increases to 0.11 mm/r. As the feed rate increases, the cutting force in the process of milling increases, and the degree of plastic deformation increases, the extent of work hardening also increases. Besides, as the increase of the feed rate (per tooth feed rate), the thermal softening change is very small and its heat effect is basically the same, so the hardening effect caused by plastic deformation is dominant.

3.3. Roughness

To study the influence of cutting parameters on surface roughness, we design a single factor experiment, arrange test line, by which the influence of different cutting parameters on the surface roughness is determined and compared.

The roughness variation with different cutting parameters is shown in Table 3. The roughness reduces with the increase of cutting speed, because when the cutting speed increases, the cutting force is reduced, and the cutting process is relatively stable, which improved the surface quality of the work piece. The

Table 3
Roughness results of the single factor experiment.

Speed (r/min)	ap (mm)	f (mm/r)	Ra (μm)
1000	1	0.05	1.736
1400	1	0.05	1.503
1800	1	0.05	1.247
2200	1	0.05	1.102
1400	0.5	0.05	1.358
1400	1	0.05	1.472
1400	1.5	0.05	1.526
1400	2	0.05	1.588
1400	1	0.02	1.375
1400	1	0.05	1.433
1400	1	0.08	1.557
1400	1	0.11	1.671

roughness increases as the depth increases, which is mainly attributed to larger removal rate in unit time and higher cutting force of the workpiece for larger cutting depth, thus imposing on larger impact for the processing system, the cutting shock between the tool and workpiece accordingly increases, resulting in deterioration of the cutting surface quality and the workpiece surface roughness finally increases. The roughness increases as the feed increases, because when the feed increases, the material removal rate in unit time of the workpiece gets larger, cutting force also increases. Like the effect of cutting depth variation, these will have a larger effect on the processing system.

3.4. Roughness model

As for high speed cutting, the research on surface quality factors requires more reliable theoretical analysis method. In order to optimize the cutting parameters and realize the accurate prediction of cutting parameters, the orthogonal cutting experiment is also designed and the roughness model formula is deduced. The experimental results are listed in Table 4.

According to some scholars, the functional relationship between roughness and the investigated independent variables could be described by the equation as following [17]:

$$Ra = C v^k a_p^m f^n \tag{1}$$

- Where Ra = roughness value
- v = cutting speed
- ap = depth
- f = feed rate
- k, m, n = regression coefficient
- C = constant

In this paper, combining the equation and Matlab, the specific procedures are given as follows:

```

X1 = [ ];
X2 = [ ];
X3 = [ ];
Y = [ ];
a = [ones(32,1),log(X1)',log(X2)',log(X3)'];
y = log(Y)';
[b,bint,r,rint,stats] = regress(y,a);
b,bint
K = exp(b(1))
    
```

Table 4
Results of the orthogonal experiment.

Order number	Speed (r/min)	ap (mm)	f (mm/r)	Ra (μm)
1	1000	0.5	0.02	1.576
2	1000	1	0.05	1.827
3	1000	1.5	0.08	1.998
4	1000	2	0.11	2.274
5	1400	0.5	0.05	1.416
6	1400	1	0.02	1.375
7	1400	1.5	0.11	1.752
8	1400	2	0.08	1.693
9	1800	0.5	0.08	1.342
10	1800	1	0.11	1.588
11	1800	1.5	0.02	1.215
12	1800	2	0.05	1.459
13	2200	0.5	0.11	1.321
14	2200	1	0.08	1.283
15	2200	1.5	0.05	1.277
16	2200	2	0.02	1.149
17	1000	0.5	0.02	1.483
18	1000	1	0.05	1.846
19	1000	1.5	0.08	2.017
20	1000	2	0.11	2.198
21	1400	0.5	0.05	1.485
22	1400	1	0.02	1.309
23	1400	1.5	0.11	1.701
24	1400	2	0.08	1.792
25	1800	0.5	0.08	1.207
26	1800	1	0.11	1.554
27	1800	1.5	0.02	1.263
28	1800	2	0.05	1.558
29	2200	0.5	0.11	1.332
30	2200	1	0.08	1.306
31	2200	1.5	0.05	1.261
32	2200	2	0.02	1.055

the model is calculated as follows:

$$Ra = 103.01924V^{-0.5197} a_p^{0.0941} f^{0.1465} \tag{2}$$

The error between this model and the actual value is calculated in Fig. 9, and the overall data is a good agreement with the residual plot except 3 points. Therefore, the fitting formula could be used for our high speed cutting of AZ31 Mg alloys.

4. Conclusions

In this study, effect of cutting parameters is investigated through the design of single factor and orthogonal experiment. It demonstrates that cutting speed, depth and feed rate have an important effect on microstructure, hardness and roughness. Besides, a geometrical model of the roughness is established. Details are concluded as follows:

- 1 The stress layer depth decreases with the increase of the cutting speed. As the speed increases from 1000r/min to 1400 r/min, the depth reduces from 40 μm to 25 μm, while it increases with the increase of feed rate. But it is not significantly changed with the depth variation.
- 2 Hardness reduces from the edge to interior at each cutting condition. The variation range is within about 20 μm. As the cutting speed increases from 1000r/min to 1400 r/min, the hardening ability decreases from 135% to 120%, whereas the hardening ability increases with the increase of cutting depth and feed rate.

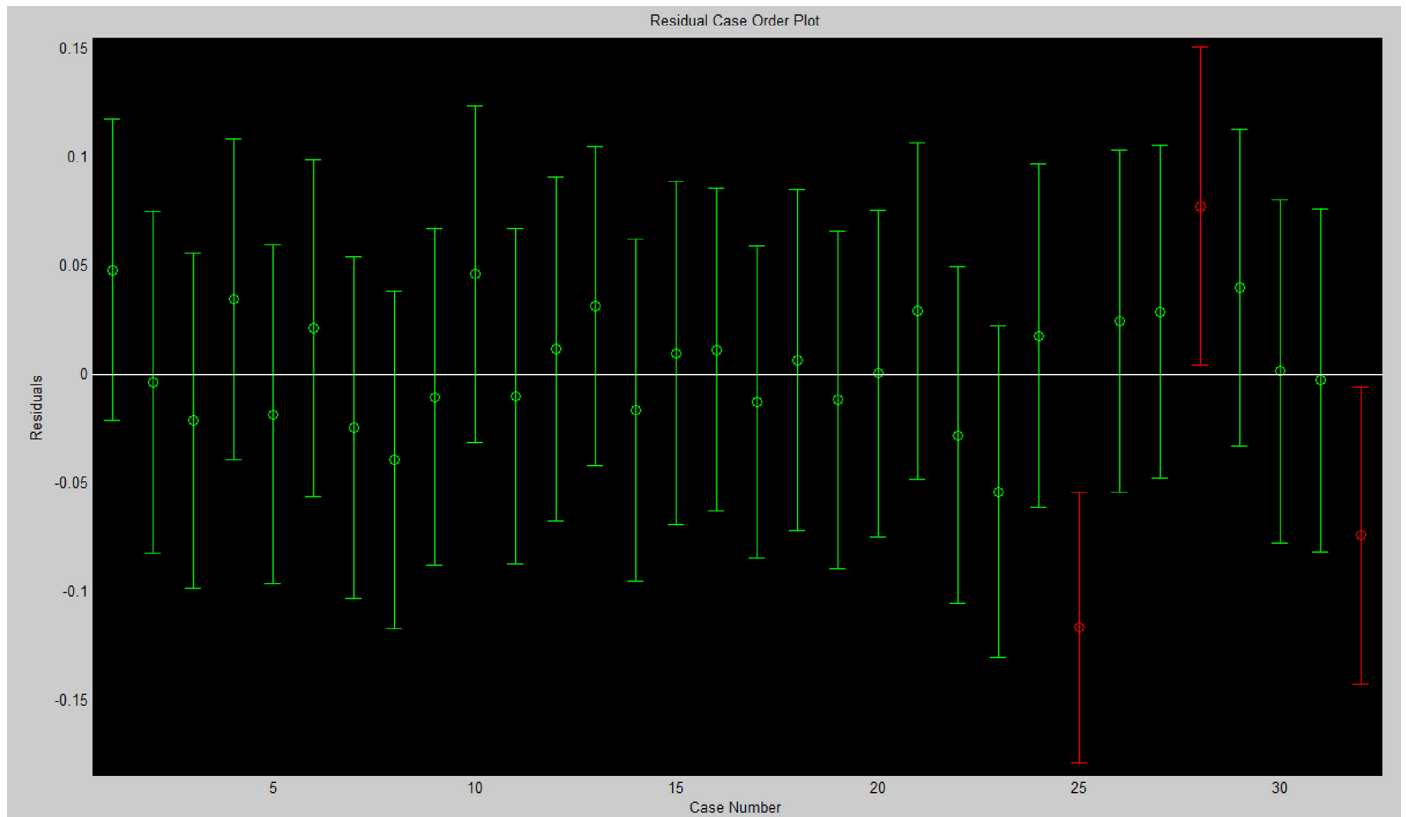


Fig. 9. The error between roughness model and actual value.

3 Roughness reduces with the increase of cutting speed, while it increases with the increase of depth and feed rate. All the variation range is within about 1 μm .

Acknowledgement

This work was supported partly by National Natural Science Foundation of China (Grant No. 51505143) and Hunan Provincial Natural Science Foundation of China (Grant nos. 14JJ3111). L.L. appreciates the financial supports from the China Postdoctoral Science Foundation (Grant No. 2014M562128) and Scientific Research Fund of Hunan Provincial Education Department (Grant no. 14C0455).

References

- [1] S.X. Sun, Y.T. Qin, H. Zhou, Y. Du, C.Y. He, J. Magnes. Alloy. 4 (2016) 30–35.
- [2] X.Y. Zhang, C. Lou, J. Tu, Q. Liu, J. Mater. Sci. Technol. 29 (2013) 1123–1128.
- [3] L.B. Tong, M.Y. Zheng, S. Kamado, D.P. Zhang, J. Meng, L.R. Cheng, et al., J. Magnes. Alloy. 3 (2015) 302–308.
- [4] M.G. Jiang, H. Yan, R.S. Chen, J. Alloys. Comp. 650 (2015) 399–409.
- [5] W.Q. Tang, S.Y. Huang, D.Y. Li, Y.H. Peng, J. Mater. Process. Tech. 215 (2015) 320–326.
- [6] T.Z. Wang, T.L. Zhu, J.F. Sun, R.Z. Wu, M.L. Zhang, J. Magnes. Alloy. 3 (2015) 345–351.
- [7] Y.B. Jiang, L. Guan, G.Y. Tang, J. Alloys. Comp. 656 (2016) 272–277.
- [8] B. Ratna Sunil, K.V. Ganesh, P. Pavan, G. Vadapalli, C. Swarnalatha, P. Swapna, et al., J. Magnes. Alloy. 4 (2016) 15–21.
- [9] A. Gómez-Parra, F.J. Puerta, E.I. Rosales, J.M. González-Madrigal, M. Marcos, Procedia Eng. 132 (2015) 513–520.
- [10] P. Sam Paul, A.S. Varadarajan, R. Robinson Gnanadurai, Eng. Sci. Tech. 19 (2016) 241–253.
- [11] K. Huang, W.Y. Yang, J. Mater. Process. Tech. 229 (2016) 375–389.
- [12] S. Karabulut, Measurement 66 (2015) 139–149.
- [13] A. Kumar, M.M. Mahapatra, P.K. Jha, Measurement 48 (2014) 325–332.
- [14] L.H. Meng, N. He, Y.F. Yang, W. Zhao, Rare. Metal. Mater. Eng. 44 (2015) 2381–2386.
- [15] H.B. Wu, S. To, J. Alloys. Comp. 629 (2015) 368–373.
- [16] X. Ai, High Speed Machining Technology, National Defense Industry Press, 2003, pp. 216–226.
- [17] M. Alauddin, M.A.E.I. Baradie, M.S.J. Hashmi, J. Mater. Process. Tech. 55 (1995) 123–127.